ELSEVIER

Long-range correlations and trends in global climate models: Comparison with real data

R.B. Govindan[a,c,*], Dmitry Vjushin[a,c], Stephen Brenner[b],
Armin Bunde[c], Shlomo Havlin[a], Hans-Joachim Schellnhuber[d]

[a] *Minerva Center and Department of Physics, Bar-Ilan University, Ramat-Gan 52900, Israel*
[b] *Department of Geography, Bar-Ilan University, Ramat-Gan 52900, Israel*
[c] *Institut für Theoretische Physik III, Justus-Liebig-Universität Giessen,
Heinrich-Buff-Ring 16, 35392 Giessen, Germany*
[d] *Potsdam Institute for Climate Impact Research, D-14412 Potsdam, Germany*

Abstract

We study trends and temporal correlations in the monthly mean temperature data of Prague and Melbourne derived from four state-of-the-art general circulation models that are currently used in studies of anthropogenic effects on the atmosphere: GFDL-R15-a, CSIRO-Mk2, ECHAM4/OPYC3 and HADCM3. In all models, the atmosphere is coupled to the ocean dynamics. We apply fluctuation analysis, and detrended fluctuation analysis which can systematically overcome nonstationarities in the data, to evaluate the models according to their ability to reproduce the proper fluctuations and trends in the past and compare the results with the future prediction. © 2001 Elsevier Science B.V. All rights reserved.

PACS: 92.60.Wc; 02.70.Hm; 92.60.Bh

Keywords: Correlations; Trends; Climate models; DFA; Scaling

1. Introduction

Recently it was found that temperature fluctuations measured at a given meteorological station exhibit long-range power law correlations with an exponent α close to 0.65 that is actually independent of the location of the station [1–3]. These results have been obtained by several methods (detrended fluctuation analysis (DFA), wavelet analysis and power spectra) for 14 meteorological stations scattered around the globe

─────────

* Corresponding author Department of Geography, Bar-Ilan University, Ramat-Gan 52900, Israel.
E-mail address: govindan@yafit.ph.biu.ac.il (R.B. Govindan).

[1–3] and confirmed in several other studies [4–6]. The persistence, characterized by the autocorrelation $C(s)$ of temperature variations separated by s days, approximately decays as

$$C(s) \sim s^{-\gamma} , \tag{1}$$

with roughly the same exponent $\gamma = 2 - 2\alpha \simeq 0.7$ for all stations considered. The range of this universal persistence law exceeds one decade, and is possibly even longer than the range of the temperature series considered. This implies two major consequences: (a) conventional methods based on moving averages cannot be used to properly separate trends from fluctuations; (b) conventional methods for the evaluation of the frequency of extreme low or extreme high temperature are based on the hypothesis, that the temperature fluctuations are essentially uncorrelated. The appearance of long range correlations sheds doubt on these methods.

The aim of this paper is to test several state-of-the-art General Circulation Models (GCM) for the power-law behavior given in Eq. (1). Among others, climate models are being used for predicting climatic changes that are believed to occur as a result of anthropogenic interference with the atmosphere. We study the following climate models: GFDL-R15-a, CSIRO-Mk2, ECHAM4/OPYC3 and HADCM3. Each model has certain unique characteristics such as the numerical methods, the type of sub-grid scale parameterizations, the spatial resolutions, and the period of integration. However, all are based on the same fundamental set of equations, all have common variables such as temperature, pressure, and precipitation, all account for increasing levels of CO_2 and all are coupled to ocean dynamics. In our study we use the simple fluctuation analysis (FA) which does not eliminate trends as well as 5 orders of DFA that can systematically eliminate trends of up to polynomials of the 4th order. Following is a brief description of the method.

2. Record analysis: fluctuation analysis and detrended fluctuation analysis

We consider a record T_i of mean monthly temperatures measured at a certain meteorological station. The index i counts the months in the record, $i = 1, 2, \ldots, N$. For eliminating the periodic seasonal trends, we concentrate on the departures of the T_i, $\Delta T_i = T_i - \bar{T}_i$, from the mean monthly temperature $\bar{T}_i$ for each calendar month i, say January, which has been obtained by averaging over all years in the temperature series. A conventional way to study correlations in the sequence ΔT_i is by the autocorrelation function:

$$C(s) = \langle \Delta T_i, \Delta T_{i+s} \rangle = \frac{1}{N-s} \sum_{i=1}^{N-s} \Delta T_i \Delta T_{i+s} . \tag{2}$$

If there is no correlation in the data, then $C(s)$ will be zero for s positive. If correlation exists up to the point s_p, then $C(s)$ will be positive up to s_p and vanish above s_p. Direct calculation of $C(s)$ is hindered by noise which is always inherent in any data, and by

possible non-stationary in the data [7]. Instead, we calculate $C(s)$ indirectly from the temperature 'profile', Y_n, which is obtained from the ΔT_i as

$$Y_n = \sum_{i=1}^{n} \Delta T_i \,. \tag{3}$$

The profile Y_n can be considered as the position of a random walker on a linear chain after n steps. The random walker starts at the origin and at the ith step makes a jump of length ΔT_i to the right if ΔT_i is positive and to the left, if ΔT_i is negative. According to random walk theory, the fluctuations $F^2(s)$ of the profile in a given time window size s, are related to the correlation function $C(s)$. For the relevant case (1) of long-range power-law correlations, $C(s) \sim s^{-\gamma}$, $0 < \gamma < 1$, the mean-square fluctuations $\overline{F^2(s)}$, obtained by averaging over many time windows of size s (see below) increase by a power law [8]:

$$\overline{F^2(s)} \sim s^{2\alpha}, \quad \alpha = 1 - \gamma/2 \,. \tag{4}$$

For uncorrelated data (as well as for correlations decaying faster than $1/s$), we have $\alpha = \frac{1}{2}$.

To determine the square-fluctuations of the profile scale with s, we first divide each record of N elements into $K_s = [2N/s]$, (indexed v) non-overlapping subsequences of size s starting from the beginning as well as from the end of the considered temperature series. We determine the square-fluctuations $F^2(s)$ in each segment v and obtain $\overline{F^2(s)}$ by averaging over all segments. On a log–log plot, the fluctuation function:

$$F(s) \equiv [\overline{F^2(s)}]^{1/2} \sim s^{\alpha} \tag{5}$$

is a straight line at large s values, with slope $\alpha > \frac{1}{2}$ in the case of long range correlations. The various methods differ in the way the fluctuation function is calculated.

2.1. Fluctuation analysis

In the simplest type of analysis (where trends are not going to be eliminated), we obtain the fluctuation functions from the values of the profile at both end points of the vth segment:

$$F_v^2(s) = [Y_{vs} - Y_{(v-1)s}]^2 \tag{6}$$

and average $F_v^2(s)$ over the K_s subsequences

$$\overline{F^2(s)} = (1/K_s) \sum_{v=1}^{K_s} F_v^2(s) \,. \tag{7}$$

Here, $\overline{F^2(s)}$ can be viewed as the mean square displacement of the random walker on a chain, after s steps. We obtain Fick's diffusion law $\overline{F^2(s)} \sim s$ for uncorrelated ΔT_i values.

We note that this fluctuation analysis corresponds to the R/S method introduced by Hurst (for a review, see e.g. [9]). Since both methods do not eliminate trends, they do not give a clear picture when used alone. In many cases they cannot distinguish

between trends and long-range correlations when applied to a time record without supplementary calculations.

2.2. Detrended fluctuation analysis

There are different orders of DFA that are distinguished by the way the trends in the data are eliminated. In the lowest order (DFA1) we determine, for each subsequence v, the best *linear* fit of the profile, and identify the fluctuations by the standard deviation $F_v^2(s)$ of the profile from this straight line. This way, we eliminate the influence of possible linear trends on scales larger than the segment sizes. Note that linear trends in the profile correspond to patch-like trends in the original record. DFA1 was originally proposed by Peng et al. [10–12] for analyzing correlations in DNA sequences and has recently been applied to the study of heartbeat dynamics [13].

DFA1 can be generalized straightforwardly to eliminate higher order trends: In second order DFA (DFA2) one calculates the standard deviations $F_v^2(s)$ of the profile from best *quadratic* fits of the profile, in this way eliminating the influence of possible linear trends on scales larger than the segment considered. In general, in the nth-order DFA technique, we calculate the deviations of the profile from the best nth-order polynomial fit and can eliminate this way the influence of the possible $(n-1)$th-order trends on scales larger than the segment size.

It is essential in the DFA-analysis that the results of several orders of DFA (e.g. DFA1–DFA5) are compared with each other. The results are only reliable when different orders yield the same type of behavior. When compared with FA one can gain additional insight into possible nonstationarities in the data.

3. Analysis of temperature records

Figs. 1a and 3a, represent the results of FA and DFA of the monthly mean temperatures T_i for the cities of Prague (1775–1992) and Melbourne (1859–1994), respectively. In the log–log plots, all curves are (except for small s-values) approximately straight lines, with slopes $\alpha = 0.65$. A natural crossover exists (above the DFA-crossover) which can be best estimated from FA and DFA1. Above the crossover, long-range persistence exists as expressed by the power-law decay of the correlation function with an exponent $\gamma \simeq 0.7$. At large time scales there is a slight increase of the FA-function for Prague(which clearly indicates a weak trend) which can be interpreted as the effect of the warming of Prague due to urban development.

As shown earlier [1–3] these results are typical for many weather stations. Since the exponent does not depend on the location of the meteorological station and its local environment, the power law behavior can serve as an ideal test for climate models where regional details cannot be resolved and therefore regional phenomena like urban warming cannot be accounted for. The power law behavior seems to be a global phenomenon and therefore should also appear in simulated data of the GCM.

3.1. Analysis of simulated temperature records

Next we consider the analysis of simulated data that were obtained from four GCMs by the interpolation of the four grid points closest to Prague and Melbourne. The models evaluated are:

1. GFDL-R15-a. This is the latest version of a coupled atmosphere-ocean model (AOGCM) that has been developed over many years at the Geophysical Fluid Dynamics Laboratory in Princeton [14,15]. The atmospheric sub-model is a spectral model with a horizontal truncation of rhomboidal 15 (R15), a transform grid longitude–latitude spacing of $7.5° \times 4.5°$, and nine vertical levels. The ocean sub-model is a grid point model with a latitude–longitude grid spacing of $4.5° \times 3.75°$ and 12 vertical layers. To reduce model drift, flux corrections are applied to the heat and water fluxes at the surface. In the control run, the CO_2 concentration is kept fixed at the 1958 value while for the climate change run all greenhouse gases are represented by equivalent CO_2 concentrations which increase at a rate of roughly 1 *percent* per year according to the IPCC IS92a scenario [16]. This model forecasts an increase of the global mean temperature by $2.2°C$ at year 2057 [17].

2. CSIRO-Mk2. The CSIRO-Mk2 model is a coupled AOGCM developed at Australia's Commonwealth Scientific and Industrial Research Organisation. The atmospheric sub-model is a spectral model with R21 truncation, a transform grid longitude–latitude spacing of $5.6° \times 3.2°$, and nine vertical layers. The ocean sub-model is a grid point model that uses the same horizontal grid as the atmosphere and has 21 vertical levels. Flux correction is applied to the heat, fresh water, and momentum fluxes at the surface. All greenhouse gases are combined into an equivalent CO_2 concentration which follows observations from 1880 to 1989 and are then projected into the future according to the IS92a scenario [18,19]. This model forecasts an increase of the global mean temperature by $3.3°C$ during the next century [17].

3. ECHAM4/OPYC3. The coupled AOGCM ECHAM4/OPYC3 was developed as a cooperative effort between the Max-Planck-Institut für Meteorologie (MPI) and Deutsches Klimarechenzentrum (DKRZ) in Hamburg. The atmospheric model was derived from the European Centre for Medium Range Weather Forecasts (ECMWF) model. It is a spectral model with triangular truncation T42, a longitude–latitude transform grid with a spacing of $2.8°$, and 19 vertical levels. The ocean model (OPYC3) is a grid point model with 11 isopycnal layers run on the same grid as the atmosphere. Flux correction is applied to the heat, fresh water, and momentum fluxes at the surface [20–22]. Historic greenhouse gas concentrations are used from 1860–1989 and from 1990 onward they are projected according to the IS92a scenario. This model forecasts an increase of the global mean temperature by $3.0°C$ during the next century [17].

4. HADCM3. The HADCM3 model is the latest version of the coupled AOGCM developed at the Hadley Centre [23]. Unlike the other models described above, here the atmospheric model is a grid point model with a longitude–latitude grid spacing of $3.75° \times 2.5°$ with 19 vertical levels. The ocean model has a horizontal resolution of $1.25°$ in both latitude and longitude and 20 vertical levels. No flux correction is
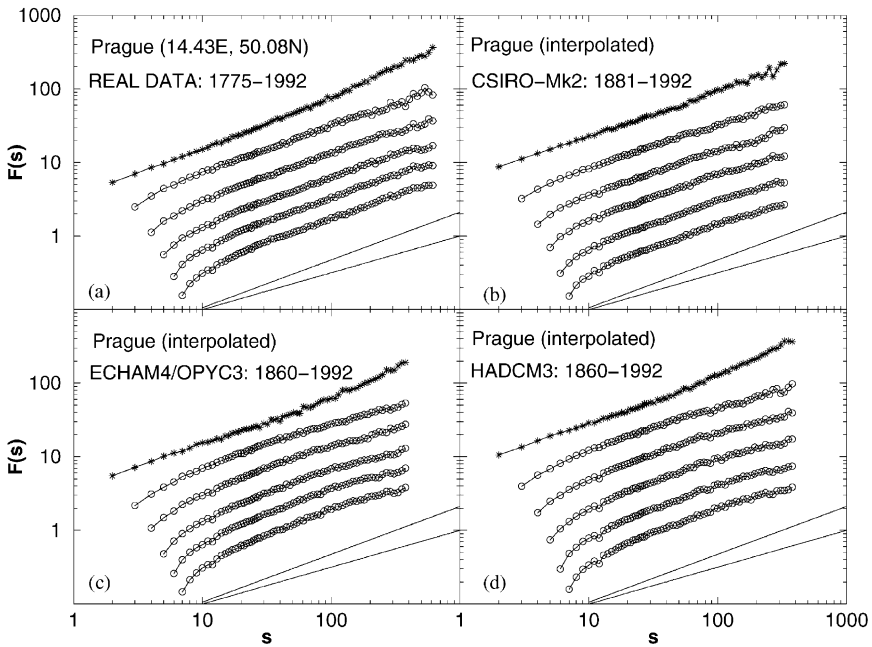
Fig. 1. FA- and DFA- of (a) the monthly mean temperature record of Prague and (b) simulated interpolated monthly mean temperature records at the geographical position of Prague, for three general circulation models: (b) CSIRO-Mk2, (c) ECHAM4/OPYC3, and (d) HADCM3. The four panels show the fluctuation functions obtained by FA, DFA1, DFA2, DFA3, DFA4, and DFA5 (from top to bottom) for the 4 sets of data. The scale of the fluctuations is arbitrary. The two straight lines at the bottom represent slopes 0.65 (upper line) and 0.5 (lower line).

applied at the surface. Historic greenhouse gas concentrations are used during the period 1860–1989. From 1990 onward they are increased according to the IS95a scenario (a slightly modified version of IS92a). This model forecasts an increase of the global mean temperature by $3.2°C$ during the next century [17].

For each model, we extracted the temperature records (mean monthly data) of the 4 grid points closest to Prague and Melbourne, from the model results obtained from the IPCC Data Distribution Centre web site [17]. The data were bilinearly interpolated to the locations of Prague and Melbourne.

Figs. 1 and 3 (b–d) show the results obtained from the segments of the ECHAM4/OPYC3, CSIRO-Mk2 and HADCM3 simulations, that end up the same year as the real record for Prague and Melbourne, respectively. The available data of GFDL-R15-a for the past cover only 40 yr, and therefore we do not present it here.

We are interested in the way the models can reproduce the actual data in terms of trends and long-range correlations. Of course, we cannot expect the models to reproduce local trends like urban warming or short-term correlation structures. But the long-range correlations as discussed in the previous section show characteristic universal features that are actually independent of the local environment around a station. Thus we can expect that successful models with good prognostic features will be able to reproduce
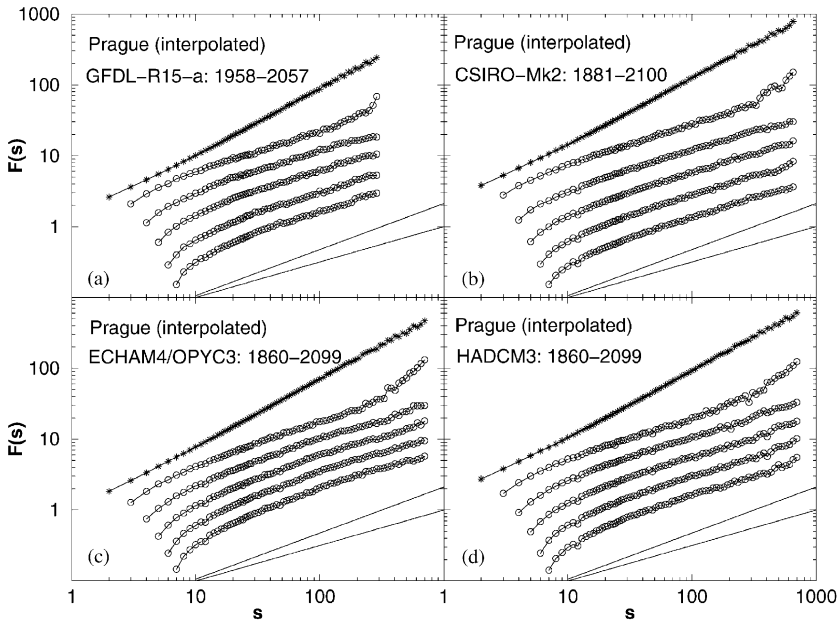
Fig. 2. FA- and DFA-analysis of the simulated interpolated monthly mean temperature records of the geographical position of Prague, for four general circulation models: (a) GFDL-R15-a, (b) CSIRO-Mk2, (c) ECHAM4/OPYC3, and (d) HADCM3. While Fig. 1 considered only data in the past, Fig. 2 considers the whole set of data up to about year 2100 (past and future).

them. Next, we present the results for Prague and Melbourne comparing the real records to the model records.

(a) Prague: The FA and DFA fluctuation functions for the real temperature record of Prague have approximately the same slope of $\alpha = 0.65$ in the double logarithmic plot (shown as straight line in Fig. 1a). At large time scales there is a slight increase in the slope of the FA—function (which clearly indicates a weak trend). In contrast, the FA—results (shown by "*") for the ECHAM4/OPYC3 (Fig. 1c) and HADCM3 (Fig. 1d) data show a stronger trend beyond 100 months represented by a larger slope. For CSIRO-Mk2 (Fig. 1b) the FA—results are not so conclusive due to the considerable scatter at large scales. Thus, it seems that two of the three models overestimate the trends of the past. Regarding scaling, the DFA curves (shown by "o") in the CSIRO-Mk2 (Fig. 1b) model show good straight line behavior in a double logarithmic presentation and yield an exponent close to the real data. In contrast, the ECHAM4/OPYC3 (Fig. 1c) and HADCM3 (Fig. 1d) models show a crossover in the fluctuation function at about 30 months with a slope close to the real data below the crossover and a slope of 0.5 above it. The exponent $\alpha = 0.5$ indicates the loss of persistence. Hence these models produce data sets which lack correlations exceeding 30 months, in contrast to the real record.

When we consider the full records (including next century data, see Figs. 2a–d), all the models show pronounced linear trends which are shown by the fluctuation functions
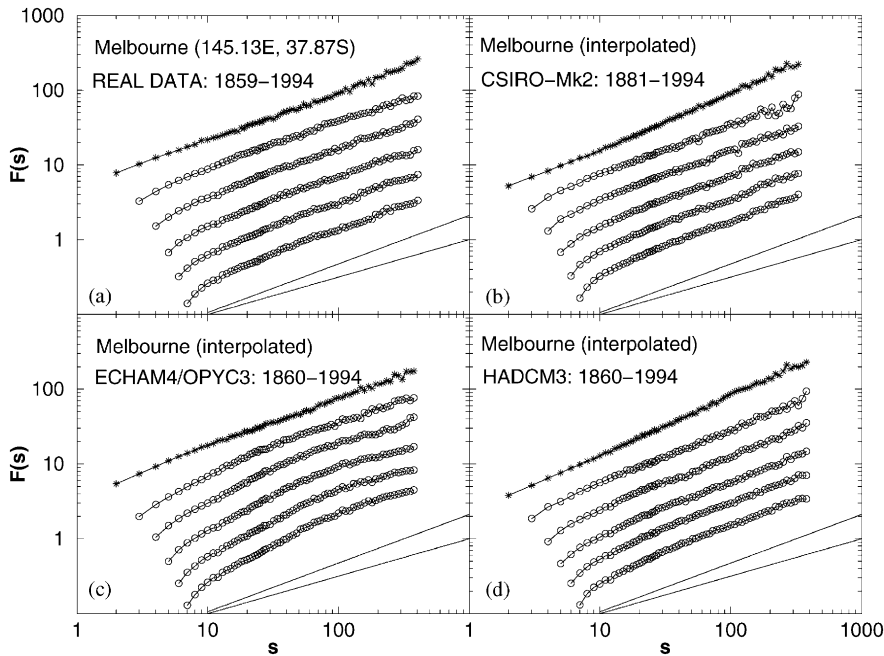
Fig. 3. Descriptions are same as that of Figs. 1 (a–d) but for Melbourne data.

obtained from FA and DFA1. Regarding scaling, all models show scaling with single exponent but yield lower exponent α between 0.5 and 0.54 when compared with real data.

(b) Melbourne: For Melbourne, the results of FA (shown by "*") for the past data (Figs. 3a–d), show that all the models slightly overestimate trends at the large time scales except the CSIRO-Mk2 (Fig. 3b) model. Regarding scaling in DFA, CSIRO-Mk2 (Fig. 3b) and HADCM3 (Fig. 3d) show straight line behavior in the double logarithmic presentation. In this case, as for Prague, CSIRO-Mk2 shows an exponent close to the real data where as the HADCM3 yields a slightly higher exponent. In contrast the ECHAM4/OPYC3 (Fig. 3c) model shows a crossover at around 30 months yielding exponents close to the real data below the crossover and 0.5 above it, again indicating the loss of persistence at large time scales.

When we consider the entire records, the linear trends in the models are stronger and might be overestimated as is clearly evident from $F(s)$ obtained from FA and DFA1 at large time scales (Figs. 4a–d). Regarding scaling behavior, ECHAM4/OPYC3 (Fig. 4c) shows a crossover at around 30 months. Below the crossover it yields a high exponent of about 0.85, while above the crossover α is about 0.6. In this case CSIRO-Mk2 and HADCM3 show similar results as for the past data.

We have also obtained similar qualitative behavior for other simulated temperature records. From the trends, one can estimate the warming of the atmosphere in future. Since the trends are almost not visible in the real data and overestimated by the
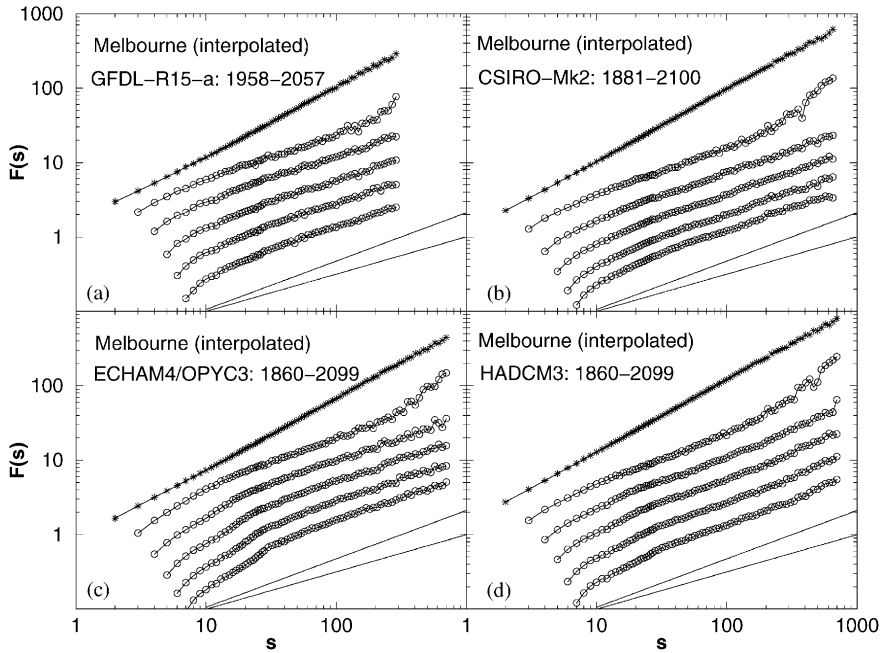
Fig. 4. Descriptions are same as that of Figs. 2 (a–d) but for Melbourne data. While Figs. 3 (a–d) considered only data in the past, Fig. 4 considers the whole data up to about year 2100 (past and future).

models in the past, it seems possible that the trends are also overestimated for the future projections of the simulations. From this point of view, it is quite possible that the global warming in the next 100 yr will be less pronounced than that is predicted by the models.

Acknowledgements

References

[1] E. Koscielny-Bunde, A. Bunde, S. Havlin, Y. Goldreich, Physica A 231 (1996) 393.
[2] E. Koscielny-Bunde, H.E. Roman, A. Bunde, S. Havlin, H.-J. Schellnhuber, Philos. Mag. B 77 (1998) 1331.
[3] E. Koscielny-Bunde, A. Bunde, S. Havlin, H.E. Roman, Y. Goldreich, H.-J. Schellnhuber, Phys. Rev. Lett. 81 (1998) 729.
[4] J.D. Pelletier, J. Clim. 10 (1997) 1331.
[5] J.D. Pelletier, D.L. Turcotte, J. Hydrology 203 (1997) 198.
[6] P. Talkner, R.O. Webber, Phys. Rev. E 62 (2000) 150.
[7] T. Schreiber, Phys. Rev. E 48 (1993) R13.
[8] A. Bunde, S. Havlin, Fractals in Science, Springer, New York, 1995.
[9] J. Feder, Fractals, Plenum Press, New York, 1989.

[10] C.-K. Peng, S.V. Buldyrev, A.L. Goldberger, S. Havlin, F. Sciortino, M. Simons, H.E. Stanley, Nature 356 (1992) 168.

[11] S.V. Buldyrev, A.L. Goldberger, S. Havlin, C.K. Peng, M. Simons, F. Sciortino, Phys. Rev. Lett. 71 (1993) 1776.

[12] S.V. Buldyrev, A.L. Goldberger, S. Havlin, R.N. Mantegna, M.E. Matsa ME, C.-K. Peng, M. Simons, H.E. Stanley, Phys. Rev. E 51 (1995) 5084.

[13] A. Bunde, S. Havlin, J.W. Kantelhardt, T. Penzel, J.H. Peter, K. Voigt, Phys. Rev. Lett. 85 (2000) 3736.

[14] S. Manabe, R.J. Stouffer, M.J. Spelman, K. Bryan, J. Climate 4 (1991) 785.

[15] S. Manabe, M.J. Spelman, R.J. Stouffer, J. Climate 5 (1992) 105.

[16] Leggett, J., W.J. Pepper, R.J. Swart, in: J.T. Houghton, B.A. Callander, S.K. Varney (Eds.), Climate Change 1992: The Supplementary Report to the IPCC Scientific Assessment, Cambridge University Press, Cambridge, Vol. 75, 1992.

[17] http://ipcc-ddc.cru.uea.ac.uk/dkrz/dkrz_index.html

[18] H.B. Gordon, S.P. O'Farrell, Mon. Wea. Rev. 125 (1997) 875.

[19] A.C. Hirst, H.B. Gordon, S.P. O'Farrell, Geophys. Res. Lett. 23 (1996) 3361.

[20] L. Bengtsson, K. Arpe, E. Roeckner et al., Clim. Dynam. 12 (1996) 261.

[21] ECHAM3: Atmospheric General Circulation Model: Editor: Dkrz-Model User Support Group, October 1996.

[22] The OPYC Ocean General Circulation Model: Joseph M. Oberhuber, October 1992, Deutsches Klimarechenzentrum (DKRZ): Report No. 7, 1997.

[23] C. Gordon, C. Cooper, C.A. Senior et al., Clim. Dynam. 16 (2000) 147.